Catalysis Today 171 (2011) 229–235

Contents lists available at ScienceDirect

Catalysis Today

journal homepage: www.elsevier.com/locate/cattod

A double-shell capsule catalyst with core–shell-like structure for one-step exactly controlled synthesis of dimethyl ether from CO_2 containing syngas

Guohui Yang[a], Montree Thongkam[b,c], Tharapong Vitidsant[b,**], Yoshiharu Yoneyama[a], Yisheng Tan[d], Noritatsu Tsubaki[a,*]

[a] Department of Applied Chemistry, School of Engineering, University of Toyama, Gofuku 3190, Toyama 930-8555, Japan
[b] Department of Chemical Technology, Faculty of Science, Chulalongkorn University, Bangkok 10330, Thailand
[c] Department of Chemistry, Faculty of Science, King Mongkut's Institute of Technology Ladkrabang, Bangkok 10520, Thailand
[d] Institute of Coal Chemistry, Chinese Academy of Sciences, Taiyuan 030001, PR China

ARTICLE INFO

Article history:
Received 31 October 2010
Received in revised form 16 February 2011
Accepted 17 February 2011
Available online 21 March 2011

Keywords:
Zeolite
Cr/ZnO catalyst
Capsule catalyst
Dimethyl ether synthesis

ABSTRACT

A zeolite capsule catalyst Cr/ZnO–S–Z was prepared successfully by a novel dual-layer method, in which one layer of neutral Silicalite-1 zeolite shell was first synthesized on the bimetallic Cr/ZnO core catalyst, acting as the intermediate layer for the following H-type H-ZSM-5 zeolite shell direct synthesis on its surface. By using this dual-layer method, it can be easily realized that the formation of H-ZSM-5 zeolite membrane on the millimeter-sized bimetallic substrates. Direct synthesis of dimethyl ether (DME) from syngas at higher reaction temperature was the application of this zeolite capsule catalyst to test its catalytic performance. In reaction, this zeolite capsule catalyst could realize the exactly controlled synthesis of DME, suppressing the formation of other alkane/alkene by-products simultaneously, demonstrating its exclusive ability for the selective synthesis of target product compared with the conventional hybrid catalyst.

1. Introduction

Dimethyl ether (DME), the simplest ether, with the simple chemical formula of $CH_3–O–CH_3$ was a potential alternative of the fossil fuels for the future [1]. It was a well-known propellant, coolant and an alternative fuel for diesel engines due to its good properties, such as its high cetane index (>55) and the low emission of CO, NOx and particulates in its combustion [2,3]. It can be also used as substitute for liquefied petroleum gas (LPG) that was widely used as fuel in industry and household now. Usually, DME can be produced by methanol dehydration over a solid acid catalyst. Here, the methanol used for DME synthesis was produced from syngas. Another way for DME synthesis was the direct conversion of syngas over a physical mixing catalyst [4–8]. The latter way, from syngas to dimethyl ether (STD), was a potential process and more favorable in views of thermodynamics and economy [9–11], which made it get more considerable attentions. Furthermore, the incorporation of CO_2 in the syngas can make the conversion from methanol to DME thermodynamically more favorable than without it, which as a positive approach also explored a new way for the large-scale utilization of CO_2. Essentially, the STD reaction consists of a series of sequential reactions: syngas to methanol, methanol dehydration to form DME, other hydrocarbons formation using DME as feedstock, and so on. The conventional hybrid catalysts for STD reaction were usually made up of methanol synthesis catalysts (such as Pd, CuO, ZnO, Al_2O_3 and/or Cr_2O_3) and methanol dehydration catalysts (such as γ-Al_2O_3 catalyst, H-Y, H-ZSM-5 or SAPOs zeolite).

For the methanol synthesis catalyst, the copper based catalyst has been widely investigated because of its high activity and moderate reaction conditions [12]. But the syngas for methanol synthesis over copper based catalyst required very low level of sulfur, chlorine and so on. Moreover, the existence of CO_2 and water in syngas can deactivate the activity of copper based catalyst more easily [13], especially under higher reaction temperature. Usually, the reaction temperature for the conversion from methanol to DME was higher than 573 K. As we know, the chromium based methanol synthesis catalyst showed more stability compared with the copper based catalyst. For methanol dehydration catalyst, zeolite catalyst such as H-Y, H-ZSM-5 zeolite catalyst having higher activity, stability occupied prominent positions in the preparation of hybrid catalyst than γ-Al_2O_3 catalyst. Until now, studies on the hybrid catalyst preparation only aimed at the simple mixing method, and a great number of physical mixing catalysts, only various in catalyst composition or reaction conditions, have been extensively investi-

---

* Corresponding author. Tel.: +81 076 4456846; fax: +81 076 4456846.
** Corresponding author.
E-mail addresses: tharapong.v@chula.ac.th (T. Vitidsant), tsubaki@eng.u-toyama.ac.jp (N. Tsubaki).

0920-5861/$ – see front matter © 2011 Elsevier B.V. All rights reserved.
doi:10.1016/j.cattod.2011.02.021

gated [5,14–17]. However, the catalyst used for this STD reaction can work more efficiently if it has a well designed core–shell structure, as proved by the present authors [18]. Furthermore, the acidic properties of solid acid catalyst may be changed when they were mixed with the metallic component.

H-ZSM-5 zeolite, an excellent catalyst due to its acidic properties [16], was often used as dehydration catalyst for methanol dehydration to form DME. The zeolite membranes constructed by zeolite crystals have more advantages than zeolite powder [19]. However, to our knowledge, it is very difficult to directly synthesize a defect-free H-type H-ZSM-5 zeolite membrane on the bimetallic substrates [20], especially for the millimeter-sized bimetallic Cr/ZnO catalyst as support. In this report, a new capsule catalyst Cr/ZnO–S–Z, for the first time, was prepared successfully using a novel dual-layer method. One layer of the neutral Silicalite-1 zeolite membrane, as the intermediate layer, was first synthesized on the bimetallic Cr/ZnO core catalyst, and then the second H-ZSM-5 zeolite membrane grew on its surface to fabricate the dual-layer final acidic zeolite shell. The illustration for the zeolite capsule catalyst Cr/ZnO–S–Z preparation process by the dual-layer method is presented in Scheme 1. The obtained zeolite capsule catalyst was used for the DME direct synthesis from syngas, and the effect of various reaction temperatures on reaction results, such as catalyst activity, product distribution, was also investigated and discussed in detail.

2. Experimental

2.1. Bimetallic catalyst preparation

The bimetallic catalyst, chromium and zinc oxide catalyst (Cr/ZnO, Cr:Zn = 1:2 in molar), used as capsule catalyst core for methanol synthesis was prepared by the conventional co-precipitation method. The appropriate amounts of metal nitrate solution and sodium carbonate solution were added dropwise over 1 h to a 300 ml of deionized water, with constant pH 9.0 at 338 K under continuous stirring, followed by 30 min ageing time to obtain the precipitates. The formed precipitates were filtered out and repeatedly washed by hot water (343 K), eliminating the effect of residual sodium ion on catalyst activity. And then it was treated by drying at 393 K for 12 h, calcination in air at 773 K for 1 h, and consequently granulating into the size of 0.85–1.70 mm. The final sample, named as Cr/ZnO catalyst, was a catalyst usually used for methanol synthesis under higher reaction temperature.

2.2. Tailor-made capsule catalyst by dual-layer method

Silicalite-1 zeolite membrane as intermediate layer was first synthesized on the surface of the bare Cr/ZnO core catalyst. The synthesis solution for its formation was of the molar composition as $0.48\text{TPAOH}:2\text{TEOS}:8\text{EtOH}:120\text{H}_2\text{O}:0.24\text{HNO}_3$. The ethanol (EtOH) and deionized water were mixed with tetrapropylammonium hydroxide (TPAOH) in a teflon container under stirring at room temperature. And then tetraethylorthosilicate (TEOS) and HNO_3 were added to the mixture respectively. After a continuous stirring at room temperature for 6 h, the obtained precursor solution and Cr/ZnO core catalyst were sealed in the teflon container by a stainless steel autoclave, loaded inside the hydrothermal synthesis instrument (DRM-420DA, Hiro Company, Japan). This hydrothermal synthesis was performed at 453 K for 24 h with a rotational speed of 2 rpm. The final samples, named as Cr/ZnO–S where “S” here indicates Silicalite-1, would be used for the following H-type ZSM-5 zeolite membrane growth on its surface.

The successive synthesis solution for H-ZSM-5 zeolite shell growth on Cr/ZnO–S support had the molar ratio of $0.48\text{TPAOH}:2\text{TEOS}:8\text{EtOH}:120\text{H}_2\text{O}:0.25\text{Al}_2\text{O}_3$. Aluminum nitrate nonahydrate ($Al(NO_3)_3{\cdot}9H_2O$, 99.9%, Wako) was selected as the aluminum resource. Other reagents and hydrothermal synthesis conditions were the same to Silicalite-1 zeolite intermediate layer preparation mentioned above, but without HNO_3 in synthesis solution. The samples after this second hydrothermal synthesis were separated from mother liquid, washed by deionized water, dried at 393 K for 12 h, and then calcined at 773 K for 5 h removing the organic template settled in zeolite pores. The final zeolite capsule catalysts were named as Cr/ZnO–S–Z, where the “Z” means the H-ZSM-5 zeolite shell. The weight increment of this capsule catalyst after this zeolite shell preparation process was about 9.7 wt%.

2.3. Physically mixed catalyst of Cr/ZnO with H-ZSM-5

The H-ZSM-5 zeolite catalyst used for hybrid catalyst preparation was prepared with the same recipe and hydrothermal conditions to that of zeolite capsule catalyst preparation. The Cr/ZnO catalyst was physically mixed well with a self-made H-ZSM-5 (Si/Al = 50) zeolite powder, granulated into the pellet size range of 0.85–1.70 mm. The new catalyst pellet (Cr/ZnO:H-ZSM-5 = 10:1 in weight) was named as Cr/ZnO–Z–M, where “M” stands for the physical mixing of Cr/ZnO with H-ZSM-5 zeolite.

2.4. Catalyst characterization

The specific surface area, pore volume and average pore diameter of catalysts were determined by nitrogen adsorption in an automatic gas adsorption system (Quantachrome Autosorb-1). Before analysis, the samples were first degassed at 573 K and 3.0 Pa for 3 h. An X-ray diffractometer (RINT 2400, Rigaku Co.) equipped with Cu Kα radiation was used to collect the XRD patterns of catalysts. Operations were performed at 40 kV and 40 mA. The physical morphology of the naked Cr/ZnO core catalyst, Cr/ZnO–S and Cr/ZnO–S–Z zeolite capsule catalyst was characterized by a scanning electron microscopy (SEM) equipped with an energy-diffusive X-ray spectroscopy (EDS) attachment (JEOL, JSM-6360LV) which could simultaneously provide the catalyst surface elemental composition information. The catalysts used for this analysis were first pretreated by an auto fine coater (JEOL, JFC-1600) to coat a platinum layer on their surface.

2.5. Catalyst activity test

A pressurized flow-type reaction apparatus with a fixed-bed stainless steel reactor (ID 8 mm) was adopted for catalyst activity test. The catalysts were loaded at the middle of reactor, dried at 523 K in a flow of nitrogen for 2 h, and then reduced in situ at 673 K in a flow of hydrogen for 3 h [21]. All the effused products from the reactor were sampled in gaseous state and first analyzed online by a gas chromatograph (Shimadzu, TCD, GC-8A) for CH_4, CO and CO_2, and then the trail gases were analyzed online using another gas chromatograph (Shimadzu, FID, GC-8A) for DME, methanol and other hydrocarbons.

The total conversion shown in Table 2 was calculated as follow:

$$\text{total conv.} = \frac{a \times \text{CO conv.} + b \times \text{CO}_2\ \text{conv.}}{a+b}$$

where “a” and “b” were the contents of CO and CO_2 in the syngas respectively.

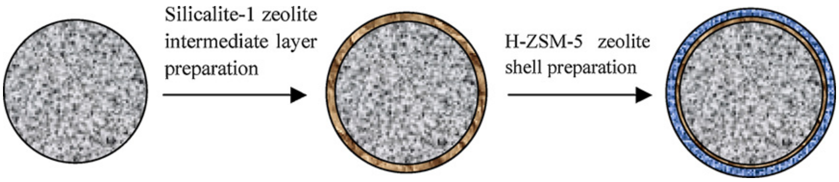

Scheme 1. Illustration of zeolite capsule catalyst preparation by using the dual-layer method.

Table 1
Physical property of catalysts.

Catalyst	Specific surface area ($m^2\ g^{-1}$)	Pore volume ($cm^3\ g^{-1}$)	Average pore diameter (nm)
Cr/ZnO	90.4	0.306	13.5
H-ZSM-5	595.6	0.308	3.4
Cr/ZnO–Z–M	148.2	0.297	10.5
Cr/ZnO–S–Z	187.8	0.222	5.9

3. Results and discussion

3.1. X-ray diffraction

X-ray diffraction is helpful to determine whether zeolite crystal was formed on the core catalyst, and what was the zeolite type. The XRD patterns of the naked Cr/ZnO catalyst, zeolite capsule catalyst Cr/ZnO–S–Z, physical mixing catalyst Cr/ZnO–Z–M and pure H-ZSM-5 zeolite are compared in Fig. 1. Comparing the XRD patterns of Cr/ZnO–S–Z with Cr/ZnO catalyst and pure H-ZSM-5 zeolite, the typical peaks belonged to pure MFI zeolite in the ranges of $2\theta = 5–10^\circ$ and 21–25° appeared, indicating that H-ZSM-5 zeolite layer had been successfully coated on the Cr/ZnO core catalyst.

3.2. BET analysis

Table 1 presents the physical properties of the bare Cr/ZnO, pure H-ZSM-5 zeolite, physical mixing catalyst Cr/ZnO–Z–M and zeolite capsule catalyst Cr/ZnO–S–Z. For zeolite capsule catalyst Cr/ZnO–S–Z, its specific surface area of 187.8 $m^2\ g^{-1}$ was larger than that of bare Cr/ZnO catalyst since the existence of zeolite shell. It was also slightly higher than that of physical mixing catalyst Cr/ZnO–Z–M, although both had the similar acidic H-ZSM-5 zeolite increment, which should be attributed to the existence of Silicalite-1 shell as intermediate layer between core catalyst and acidic H-ZSM-5 zeolite shell. Furthermore, the zeolite capsule catalyst Cr/ZnO–S–Z had lower pore volume and pore diameter, comparing with the naked Cr/ZnO catalyst and physical mixing Cr/ZnO–Z–M catalyst. For this phenomenon, the hydrothermal synthesis for this zeolite capsule catalyst preparation should be the main reason. During the hydrothermal synthesis process, few of zeolite synthesis solution entered the pores of Cr/ZnO core catalyst, and then formed some aluminosilicate that might fill a part of the pore volume and decrease the pore diameter of zeolite capsule catalyst.

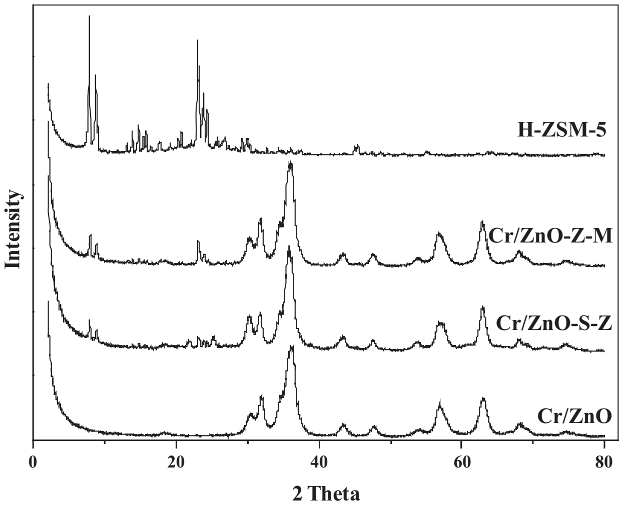

Fig. 1. XRD patterns of Cr/ZnO, Cr/ZnO–S–Z, Cr/ZnO–Z–M and pure H-ZSM-5 zeolite powder.

3.3. SEM and EDS analysis of catalysts

Fig. 2 presents the surface SEM and EDS analysis result of the naked Cr/ZnO core catalyst. Only Cr Kα and Zn Kα signals, 32.73% and Zn 67.27% respectively in molar base, can be found on the Cr/ZnO core catalyst surface, and they are close to the original bulk

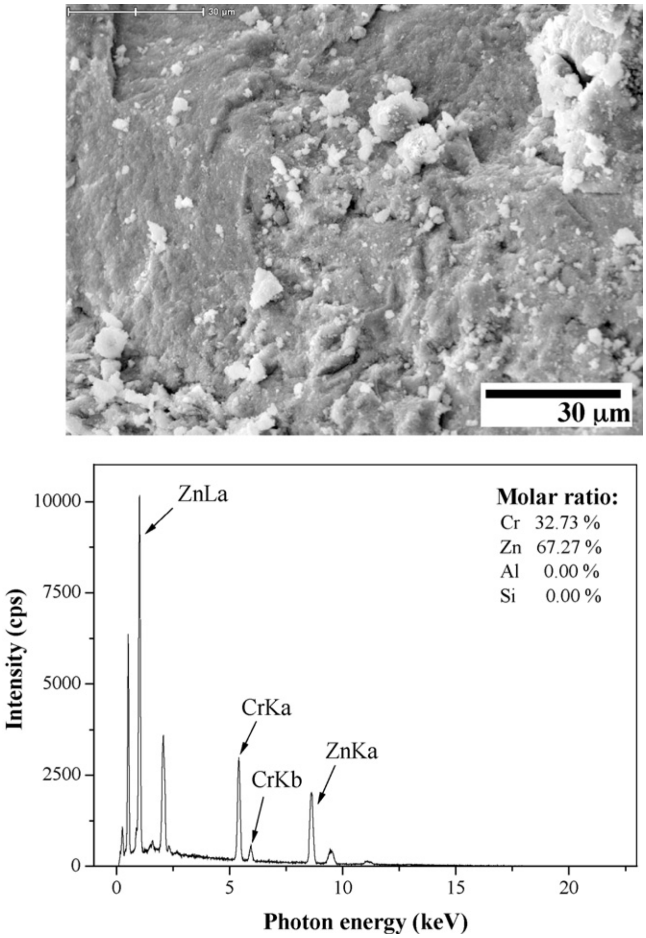

Fig. 2. Surface SEM image of the Cr/ZnO pellet and its EDS surface analysis result. Molar ratio: Cr 32.73%, Zn 67.27%, Al 0.00%, Si 0.00%.

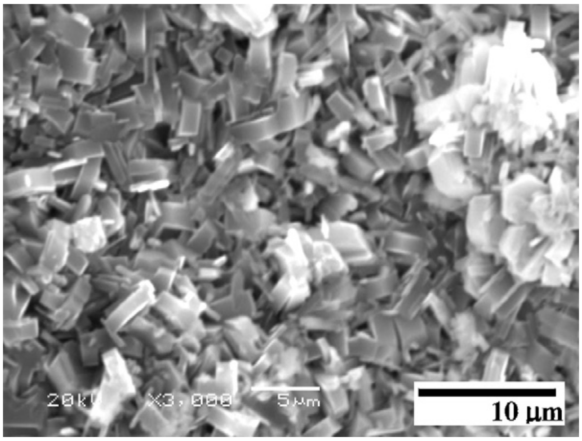

Fig. 3. Surface SEM image of the Cr/ZnO–S pellet.

ratio of catalyst preparation recipe. After the coating of Silicalite-1 zeolite shell onto the naked Cr/ZnO core catalyst, the formed Cr/ZnO–S pellet surface is covered by an integrated, uniform zeolite membrane shown in Fig. 3. Here, the formed intermediate zeolite layer of Silicalite-1 of Cr/ZnO–S can induce the growth of the followed H-ZSM-5 zeolite shell on its surface effectively, and at the same time avoid the further damage from hydrothermal synthesis as much as possible, because pH value of H-ZSM-5 zeolite synthesis mother liquid is remarkably higher than that of Silicalite-1.

The Cr/ZnO–S–Z zeolite capsule catalyst was prepared by using the second hydrothermal synthesis, constructing H-ZSM-5 zeolite shell on the surface of Cr/ZnO–S catalyst. The surface SEM and EDS analysis results of Cr/ZnO–S–Z are shown in Fig. 4. Slight differences between this H-ZSM-5 shell and the intermediate layer of Silicalite-1 zeolite shell (Fig. 3) with respect to their zeolite crystal's size and shape can be found clearly, which should be due to the dissimilar pH values of these two zeolite membranes synthesis solution [18], as well as the existence or not, of aluminum resource in their synthesis recipes [22,23]. The surface EDS analysis of Cr/ZnO–S–Z determined its surface elemental composition as in Fig. 4, where the zero intensity of Cr Kα and Zn Kα signals indicated that the zeolite shell was integrity and defect-free, suggesting that this dual-layer zeolite capsule catalyst preparation on the bimetallic core catalyst was successful. Moreover, the surface Si/Al ratio, Si/Al = 48, of this H-ZSM-5 zeolite shell can be also obtained according to this EDS analysis result.

Fig. 5 exhibits the cross-section SEM image and EDS line analysis of Cr/ZnO–S–Z zeolite capsule catalyst. From the SEM image, a compact and defect-free zeolite shell enwrapping the Cr/ZnO core catalyst can be observed clearly, which also proves that the zeolite shell synthesis on the bimetallic Cr/ZnO catalyst by this dual-layers method is successful. The EDS analysis was performed along the line in the SEM image, as shown in Fig. 5. The analysis result exhibited the change of Al Kα, Si Kα, Cr Kα and Zn Kα signals in intensity from the core catalyst to zeolite shell. At the interface region between core catalyst and zeolite shell, the radial distribution of Si Kα increased sharply while that of the Cr Kα and Zn Kα changed into zero, which demonstrated the phase change from core catalyst to zeolite shell. It should also be noted that the Al Kα signal was not zero at the zone of core catalyst which was near the zeolite shell. It is clear that some synthesis solution soaked into the outer surface of core catalyst during the hydrothermal synthesis process, and the soaked synthesis solution containing aluminum resource should contribute to this gradient. The zeolite shell thickness of Cr/ZnO–S–Z was about 9.4 μm that can be also identified according to these EDS radial distribution profiles, as displayed in Fig. 5.

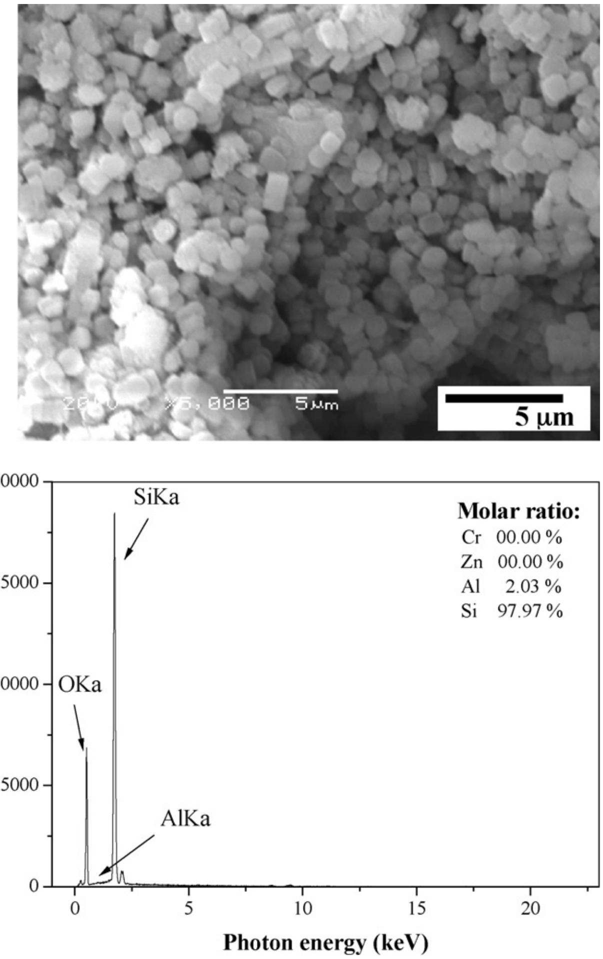

Fig. 4. Surface SEM image of the Cr/ZnO–S–Z pellet and its EDS surface analysis result. Molar ratio: Cr 0.00%, Zn 0.00%, Al 2.03%, Si 97.97%.

3.4. *Catalytic performance of catalysts in STD reaction*

The catalytic performances of the bare Cr/ZnO core catalyst, physical mixing Cr/ZnO–Z–M catalyst and zeolite capsule catalyst Cr/ZnO–S–Z prepared by the dual-layer method are compared in Table 2. The time on stream of different catalysts as a function of reaction temperature had also been presented in Fig. 6. All the catalysts were tested with the $W_{\mathrm{Cr/ZnO}}/F_{\mathrm{Syngas}} = 13.6\ \mathrm{g\ h\ mol^{-1}}$, system pressure 5.0 MPa and at varied reaction temperatures (573 K, 598 K, 623 K). The syngas used as feedstock had the composition of Ar 3.02%, CO 32.6%, CO_2 5.16%, H_2 59.22% in molar base.

For the naked Cr/ZnO catalyst, the CO conversion exhibited a linear increment with the increase of reaction temperature shown in Table 2. At 573 K, the CO conversion was only 5.43%, and then it reached 7.68% when the reaction temperature up to 623 K. A similar change also happened on Cr/ZnO–Z–M and Cr/ZnO–S–Z catalyst. Especially for the hybrid catalyst Cr/ZnO–Z–M, its CO conversion of 45.16% at higher reaction temperature of 623 K was five times more than the 9.30% at lower reaction temperature of 573 K. The higher reaction temperature, however, adversely promoted the CO_2 conversion, indicating that higher reaction temperature accelerated the Water-Gas-Shift (WGS) reaction to generate CO_2 [16].

The zeolite capsule catalysts Cr/ZnO–S–Z presented lower catalyst activities than the naked Cr/ZnO catalyst or hybrid catalyst Cr/ZnO–Z–M. For this zeolite capsule catalyst, few zeolite crystals formed during hydrothermal synthesis process covered part of the active sites of the Cr/ZnO core catalyst, which resulted in the lower catalyst activity of zeolite capsule catalyst compared with

Table 2
Reaction performance of catalysts at various reaction temperatures.[a]

Catalyst	Reaction temp. (K)	Conversion (%)			Selectivity (%)								
		CO	CO_2	Total	CH_4	C_2H_4	C_2H_6	C_3H_6	C_3H_8	MeOH	DME	C_4H_{10}	Others
Cr/ZnO	573	5.43	3.38	5.15	2.42	1.60	0.00	0.00	8.54	87.44	0.00	0.00	0.00
	598	7.26	0.48	6.33	7.79	1.06	0.00	0.56	8.91	81.04	0.64	0.00	0.00
	623	7.68	−5.43	5.89	14.22	4.57	0.00	1.72	12.47	63.74	3.40	0.00	0.00
Cr/ZnO–Z–M[b]	573	9.30	−9.42	6.74	4.41	42.01	0.00	9.62	11.15	16.06	11.12	0.00	5.63
	598	25.25	−64.96	12.93	3.96	23.77	0.00	6.42	4.74	12.75	0.81	17.40	30.15
	623	45.16	−122.21	22.29	7.65	7.34	0.00	2.69	4.58	12.12	0.47	27.34	37.81
Cr/ZnO–S–Z[c]	573	2.27	6.97	2.91	7.78	8.07	0.00	2.39	0.72	35.62	45.42	0.00	0.00
	598	6.03	0.04	5.21	4.83	7.26	0.00	7.10	0.88	34.20	45.74	0.00	0.00
	623	9.53	−14.70	6.22	11.31	7.87	0.00	6.76	1.99	21.23	50.84	0.00	0.00

[a] Reaction conditions: $W_{Cr/ZnO}/F_{Syngas} = 13.6\,g\,h\,mol^{-1}$, 5.0 MPa, 5 h; Syngas composition: Ar 3.02%, CO 32.6%, CO_2 5.16%, H_2 59.22%.

[b] "Z" stands for the H-ZSM-5 zeolite (Si/Al = 50), and the "M" means the physical mixing of Cr/ZnO with H-ZSM-5 zeolite.

[c] "S" means that the Silicalite-1 zeolite intermediate layer and "Z" the H-ZSM-5 shell.

the Cr/ZnO and Cr/ZnO–Z–M catalyst. Another factor, the "speed-down" for syngas diffusing through zeolite shell, should also be considered. The bare catalyst was enwrapped by dual-layer zeolite shells. In order to react on the zeolite capsule catalyst core, syngas must first pass through the zeolite shells, which may lead to the diffusion restrictions, comparing with that of the traditional catalyst Cr/ZnO and hybrid Cr/ZnO–Z–M catalyst. However, increasing the metal content of the core catalyst or extending the contact time of the reactant with zeolite capsule catalyst can overcome it easily.

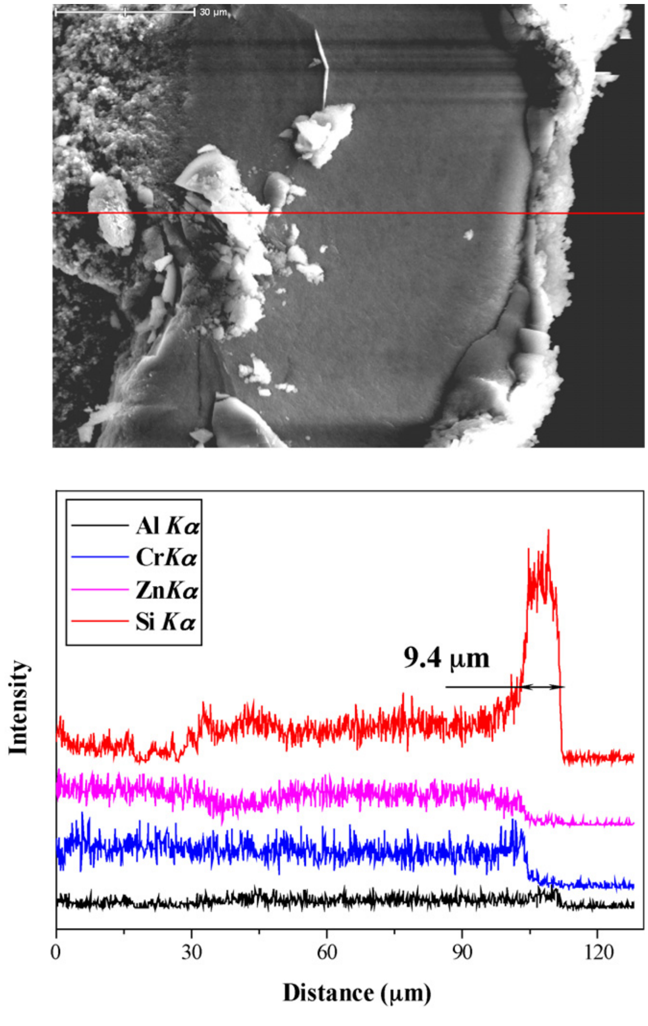

Fig. 5. Cross-sectional SEM image and the EDS line analysis of zeolite capsule catalyst Cr/ZnO–S–Z.

It should also be mentioned that, at 623 K, the catalyst activity of this zeolite capsule catalyst was better than that of the naked Cr/ZnO catalyst. Here, the promoted catalyst activity should be attributed to the shifted reaction equilibrium. It is well known that, different from the single methanol synthesis reaction happened on the naked Cr/ZnO core catalyst, on the single zeolite capsule catalyst there were a series of sequential reactions. The reaction speed of methanol synthesis from syngas occurred on the core catalyst was significantly affected by the followed DME formation from methanol dehydration on the zeolite shell, especially at higher reaction temperature. Removal of the formed methanol to DME enhanced the CO conversion for the capsule catalyst.

The product selectivity on naked Cr/ZnO, hybrid catalyst Cr/ZnO–Z–M and zeolite capsule catalyst Cr/ZnO–S–Z are also presented in Table 2. For the naked Cr/ZnO catalyst, the major component of its products was methanol. Moreover, the changes of the products distribution were obvious with the increase of reaction temperature, whereas DME always emerged as a tiny component and increased slightly along with other hydrocarbon by-products (C1–C3).

For the physical mixing catalyst Cr/ZnO–Z–M, it was made of the traditional methanol synthesis catalyst Cr/ZnO and the methanol dehydration catalyst H-ZSM-5 zeolite. Different from the naked Cr/ZnO catalyst, this hybrid catalyst had a different products distribution. The methanol selectivity on this hybrid catalyst was obviously lower than that of the naked Cr/ZnO at each reaction temperature, as in Table 2. However, DME was still the tiny products, and the major components on this hybrid catalyst were alkanes and alkenes. Considering the structure composition of this hybrid catalyst, in STD reaction, the syngas reacted first on the Cr/ZnO active sites of hybrid catalyst to form methanol, and then a part of the formed methanol might be randomly converted into DME on the zeolite active sites near the Cr/ZnO catalyst part in hybrid catalyst. The formed DME from methanol dehydration could be further converted into hydrocarbons on the zeolite active sites of one hybrid catalyst particles or another neighboring one, since it diffused freely without any spatial restriction, especially at higher reaction temperatures. The remaining methanol would continue its route to pass through the catalyst bed layer, might be not converted to DME, without contact with zeolite. This hybrid catalyst structure, with only a simple mixing, decided that only a random not ordered sequential reaction process took place. There were no an effective restriction to stop DME diffusing back into the hybrid catalyst again. As a result, alkanes and alkenes became the major products when this hybrid catalyst was used.

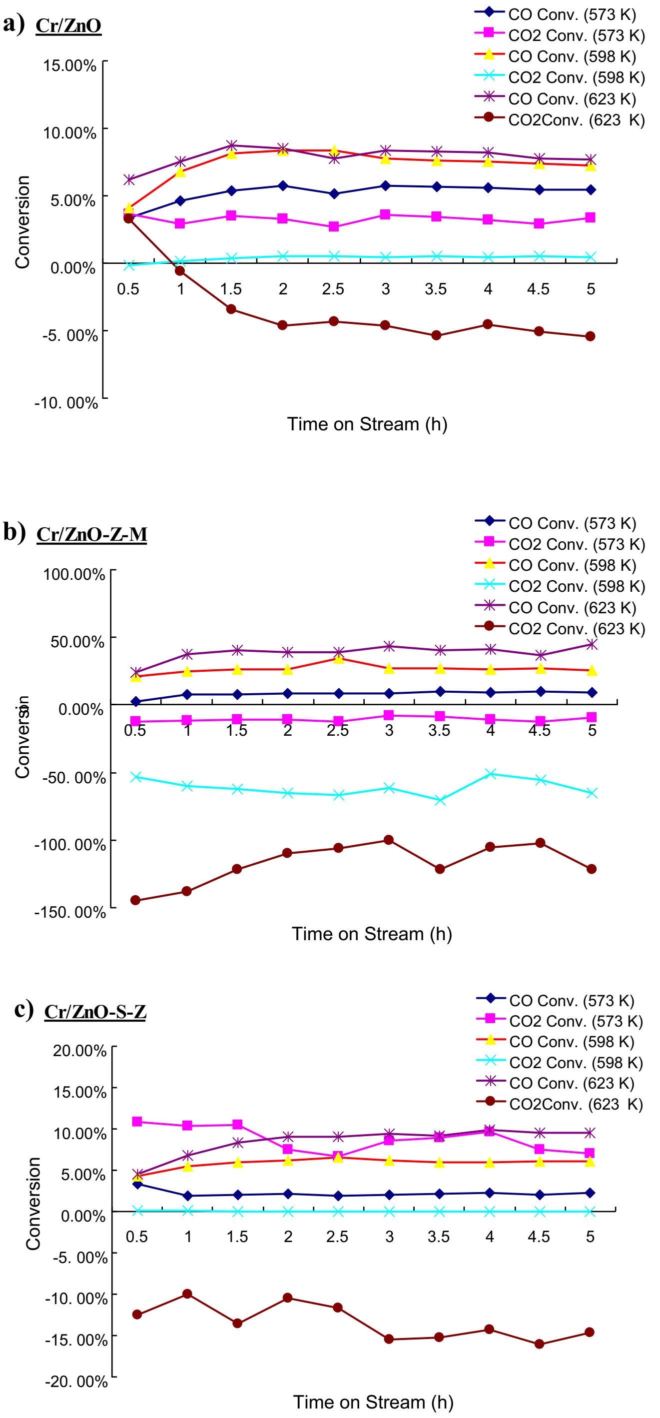

Fig. 6. Time on stream of STD reaction over different catalysts as a function of reaction temperature: (a) Cr/ZnO, (b) Cr/ZnO–Z–M and (c) Cr/ZnO–S–Z.

Different from the naked Cr/ZnO catalyst and hybrid catalyst Cr/ZnO–Z–M, zeolite capsule catalyst Cr/ZnO–S–Z gave a very dissimilar product distribution in Table 2. DME accounted for the largest proportion in the final products with alkanes and alkenes as the tiny by-products. The selectivity of DME increased from 45.42% to 50.84% as the increase of reaction temperature from 573 K to 623 K, while the selectivity of methanol decreased correspondingly. Here, the exactly controlled DME synthesis from syngas, without the formation of C4+ hydrocarbons, should be attributed to the unique core–shell structure of the zeolite capsule catalyst. For hybrid catalyst Cr/ZnO–Z–M, there were no spatially confined effect and steps restrictions between the methanol synthesis, methanol dehydration and DME dehydration to hydrocarbon reactions. The construction manner of hybrid catalyst, simply mixing, decided that the sequential reactions will only happen randomly on the two active sites of hybrid catalyst. The formed DME left the hybrid catalyst by diffusion, but it can also diffuse freely without any limitation back into the same or another hybrid catalyst to undergo further reaction transforming into other hydrocarbons. As a result, a series of sequential reactions happened on this hybrid catalyst without any restriction or order. They cannot be controlled well, stopped in hand, ended at the DME formation. The further conversion of DME to form hydrocarbons on this hybrid catalyst is very easier at least under the used reaction conditions.

However, it is entirely different for zeolite capsule catalyst Cr/ZnO–S–Z. This zeolite capsule catalyst has a special core–shell structure, in which the catalyst shell enwrapped core catalyst tightly. In STD reaction, each reaction of the sequential reactions will be restricted in the designated location. Methanol was synthesized from syngas on the core catalyst and then it would be transformed into DME on zeolite shell, followed by DME escaping from capsule catalyst. For DME dehydration, the zeolite shell with the fixed position and homogeneous property was an equal opportunity provider to each methanol molecular diffused from the core catalyst, converting them into DME concertedly, while lessening the probability of the further dehydration of DME generating alkanes/akenes. The effused DME from capsule catalyst will join the flowing syngas. The diffusion of DME back to capsule catalyst, if DME want to do that, can be effectively suppressed by zeolite shell especially in the case of competing with syngas ($CO + H_2 + CO_2$), which will obviously decrease the possibility of DME further conversion, leading to the higher DME selectivity in the final products.

Benefitting from the well-confined core–shell structure, this zeolite capsule catalyst can concertedly settle each reaction of the sequential reactions in the designated location and stop them at the desired step according to the catalyst designer's wishes. All these results indicated that the concept of this zeolite capsule catalyst was very effective and available for the controlled synthesis of target products with high selectivity, especially in the catalytic process containing a series of sequential reactions.

4. Conclusions

The acidic H-ZSM-5 shell was successfully coated on the surface of bimetallic Cr/ZnO catalysts by using an improved dual-layer method, where one layer of neutral Silicalite-1 membrane was first synthesized on the core catalyst as the intermediate layer for the followed H-ZSM-5 shell growth on its surface. Characterization on the zeolite capsule catalyst prepared by this dual-layer method indicated that the zeolite shell was compact, integrated and defect-free, suggesting that this dual-layer method was reliable for H-ZSM-5 zeolite shell synthesis on the bimetallic core catalyst. The direct synthesis of DME from syngas was the application of this zeolite capsule catalyst Cr/ZnO–S–Z, where it exhibited better performance for DME exactly controlled synthesis than the naked Cr/ZnO catalyst and physical mixing catalyst Cr/ZnO–Z–M. The dual-layer zeolite shell preparation method and zeolite capsule catalyst application, reported here, should have more potential applications not only to the zeolite capsule catalyst design and the sequential reaction processes, but also for the study of zeolite membrane.

References

[1] W. Xia, V. Hagen, S. Kundu, Y. Wang, C. Somsen, G. Eggeler, G. Sun, G. Grundmeier, M. Stratmann, M. Muhler, Advanced Materials 19 (2007) 3648–3652.

[2] Y. Adachi, M. Komoto, I. Watanabe, Y. Ohno, K. Fujimoto, Fuel 79 (2000) 229–234.
[3] G. Cai, Z. Liu, R. Shi, H. Changqing, L. Yang, C. Sun, Y. Chang, Applied Catalysis A: General 125 (1995) 29–38.
[4] M.T. Xu, D.W. Goodman, A. Bhattacharyya, Applied Catalysis A: General 149 (1997) 303–309.
[5] K. Fujimoto, K. Asami, T. Shikada, H. Tominaga, Chemistry Letters 13 (1984) 2051–2054.
[6] G.J. Hutchings, P. Johnston, Applied Catalysis 67 (1990) L5–L9.
[7] J. Khom-In, P. Praserthdam, J. Panpranot, O. Mekasuwandumrong, Catalysis Communications 9 (2008) 1955–1958.
[8] Q. Sun, Y.C. Fu, H.X. Yang, A. Auroux, J.Y. Shen, Journal of Molecular Catalysis A: Chemical 275 (2007) 183–193.
[9] K.L. Ng, D. Chadwick, B.A. Toseland, Chemical Engineering Science 54 (1999) 3587–3592.
[10] X.D. Peng, B.A. Toseland, P.J.A. Tijm, Chemical Engineering Science 54 (1999) 2787–2792.
[11] P.S.S. Prasad, J.W. Bae, S.H. Kang, Y.J. Lee, K.W. Jun, Fuel Processing Technology 89 (2008) 1281–1286.
[12] X. Guo, D. Mao, G. Lu, S. Wang, G. Wu, Journal of Catalysis 271 (2010) 178–185.
[13] I. Melián-Cabrera, M.L. Granados, J.L.G. Fierro, Journal of Catalysis 210 (2002) 285–294.
[14] D. Mao, W. Yang, J. Xia, B. Zhang, Q. Song, Q. Chen, Journal of Catalysis 230 (2005) 140–149.
[15] F.S.R. Barbosa, V.S.O. Ruiz, J.L.F. Monteiro, R.R. de Avillez, L.E.P. Borges, L.G. Appel, Catalysis Letters 126 (2008) 173–178.
[16] A.C. Sofianos, M.S. Scurrell, Industrial & Engineering Chemistry Research 30 (1991) 2372–2378.
[17] A. Venugopal, J. Palgunadi, J.K. Deog, O.-S. Joo, C.-H. Shin, Journal of Molecular Catalysis A: Chemical 302 (2009) 20–27.
[18] G. Yang, N. Tsubaki, J. Shamoto, Y. Yoneyama, Y. Zhang, Journal of the American Chemical Society 132 (2010) 8129–8136.
[19] A. Feller, A. Guzman, I. Zuazo, J.A. Lercher, Journal of Catalysis 224 (2004) 80–93.
[20] G. Yang, X. Zhang, S. Liu, K.L. Yeung, J. Wang, Journal of Physics and Chemistry of Solids 68 (2007) 26–31.
[21] Q. Zhang, X. Li, K. Fujimoto, Applied Catalysis A: General 309 (2006) 28–32.
[22] A.E. Persson, B.J. Schoeman, J. Sterte, J.E. Otterstedt, Zeolites 14 (1994) 557–567.
[23] A.E. Persson, B.J. Schoeman, J. Sterte, J.E. Otterstedt, Zeolites 15 (1995) 611–619.